

AATSR burned area limitation estimates within the FIRE-CCI project

Renata Libonati ¹
Alberto W. Setzer ¹
Emilio Chuvieco ²

¹ Instituto Nacional de Pesquisas Espaciais - INPE
Caixa Postal 515 - 12227-010 - São José dos Campos - SP, Brasil
{renata.libonati, alberto.setzer}@cptec.inpe.br

² Departamento de Geografía, Universidad de Alcalá
Colegios 2 – 28801 Alcalá de Henares (Madrid) España
Emilio.chuvieco@uah.es

Abstract. The European Satellite Agency (ESA) started a research line towards the development of operational procedures to generate global maps of burnt areas based on data from various European Earth Observation (EO) satellite instruments (AATSR, VGT and MERIS) under the scope of the Fire Disturbance project (Fire-CCI). In this context, the objective of the Round-Robin (R-R) Exercise is to compare the burned area (BA) products of algorithms from different groups and identify the best results. This paper describes INPE' burned area approach for the Round Robin exercise of the Fire-CCI project, as part of the cooperation between INPE and the University of Alcalá de Henares, Spain. Our results show the limitations and drawbacks of the provided dataset, which considerably reduces their application over burned areas.

Key-words: remote sensing, burned area algorithm, area queimada,

1. Introduction

The European Satellite Agency (ESA) has started a new line of research towards the development of operational procedures to generate global maps of burnt areas based on data provided from various European Earth Observation (EO) satellite instruments (AATSR, VGT and MERIS) under the scope of the Fire Disturbance project (Fire-CCI). In such context, the FIRE-CCI team devised the so-called Round-Robin (R-R) Exercise, aiming to compare the burned area (BA) products from different external algorithms and identify the best performing internal and external algorithm. The R-R exercise provides a common dataset to all the participants in order to assure that the burned area algorithms are applied under the same initial conditions. More information about the R-R exercise and the FIRE-CCI project may be found at <https://www.esa-fire-cci.org/>. Within the scope of a cooperation between INPE and the FIRE-CCI project, the present work describes INPE' burned area approach for the R-R exercise and the results obtained with AATSR imagery.

The INPE initiative consists on the application of the so-called “V,W” burned index (Libonati et al., 2011) to the AATSR characteristics in order to derive burnt area maps to the study site located in a predominately Cerrado (Savanna) region in central Tocantins, Brazil; for more details about the test sites see Chuvieco et al. (2011a).

An overview is given of results obtained, focusing on the limitations and drawbacks of the provided dataset.

2. Method and data set

2.1 Data set

The R-R dataset used by INPE is focused on the study site located in Brazil (Figure 1) for the years of 2005 (totalizing 144 images) and 2006 (totalizing 143 images) with the AATSR sensor. The data package offered by the FIRE-CCI project includes the pre-processed images of the AATSR sensors at 1km spatial resolution, delivered in standard GeoTiff format (TIF)

and georeferenced in UTM coordinates to the central zone of the study site. The data package used in this work consists of:

- a) Atmospheric corrected ortho-image (Q.1): bands 3 (0.87 μm), 5 (3.7 μm) and 6 (11 μm)
- b) Water mask (OWM.1):
- c) Cloud/shadow/snow/haze-mask (OCM.1)
- d) Sun angles (Qsun.1)
- e) Observation angles (Qsca.1)

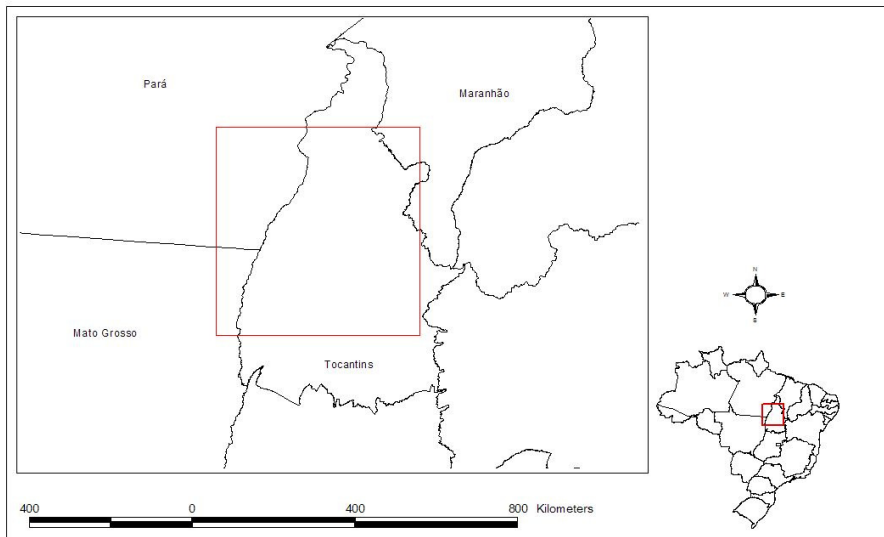


Figure 1. The Round-Robin study area located in Central Brazil (in red).

2.2 Method

The procedure is based on the (V,W) burned index developed by Libonati et al., 2011. The index was designed for the 1km MODIS Level 1B calibrated radiance data from bands 2 (near-infrared – NIR, centered at 0,856 μm) and 20 (middle-infrared – MIR, centered at 3.96 μm). In this work, we have adapted the “V,W” burned index to the AATSR characteristics using the response functions of the NIR and MIR bands, respectively, band 3 (centered at 0.87 μm) and band 5 (centered at 3.7 μm).

The algorithm detects persistent changes during a period of 10 days in the “V,W” burned index time series. The day of maximum change is then identified by means of a discrimination index, together with thresholds from the (V,W) time series. A spatial filter is finally applied to remove outliers.

Valid AATSR daily band 3 (0.87 μm) reflectances, and band 5 (3.7 μm) and band 6 (11 μm) brightness temperatures were extracted from the R-R atmospheric corrected ortho-images (Q.1) data base. To be considered valid, each daily reflectance and brightness temperature data must meet the following criteria:

- a) The pixel must be located on land, as flagged in the Water Mask (OWM.1). For both static and dynamic water masks inside OWM.1, we considered as land those pixels with static or dynamic water mask equal to zero%.
- b) The observation must be free from cloud, shadow, snow and haze contamination, as flagged in the Cloud/Shadow/Snow/Haze-Mask dataset (OCM.1). The OCM.1 dataset provides confidence levels for contamination of cloud in band 1, snow in band 2, cloud-shadow in band 3 and haze in band 4.. For instance, if Band_x = 100, the pixel is cloudy in band 1, cloud-shadow in band 3, snow in band 2, or haze in band 4. On

the other hand, if $\text{Band}_x = 0$, the pixel is surely not cloudy, cloud-shadow, snow, haze. In the case that $\text{Band}_x = 50$ it is uncertain that the pixel can be declared as cloudy, cloud-shadow, snow, haze.

- c) The observation scan angle must be less than 45 degrees in the Observation Angles (Qsca.1) Dataset, in order to avoid pixel size degradation.
- d) The sun zenith angle must be less than 60 degrees, as in Sun Angles (Qsun.1) Dataset, in order to avoid problems in MIR reflectance, as pointed out by Libonati et al., 2010.

Figure 2 shows an example of the above mentioned sequence applied to band 3.

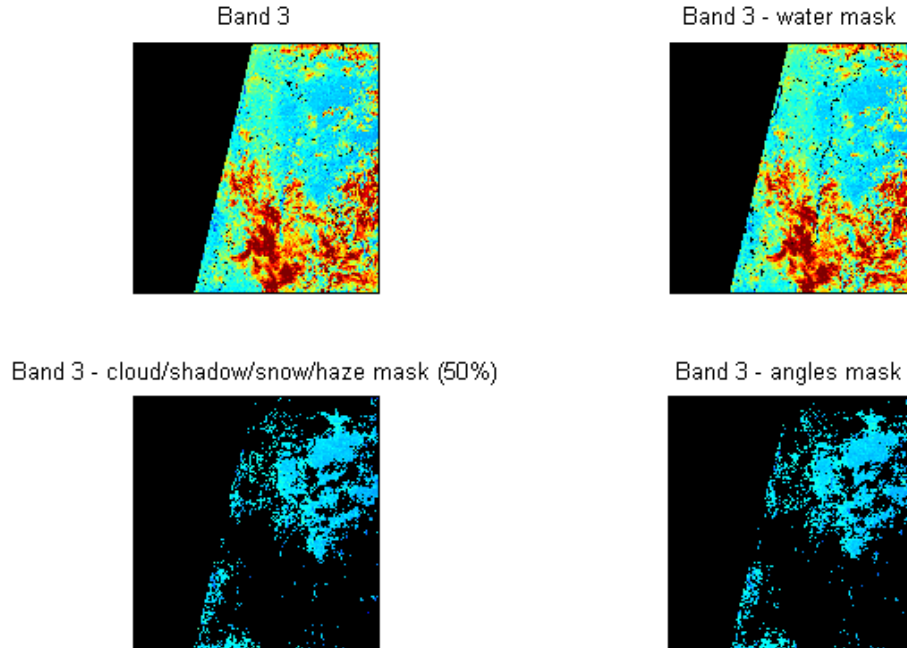


Figure 2. Example of the applied conditions used to select valid pixels for 11-Feb-2005 (dd-mm-yy). Upper left panel: band 3. Upper right panel: band 3 with water mask. Lower left panel: band 3 with cloud/shadow/snow/haze mask applied for pixels with more than 50% of confidence level. Lower right panel: sun and observation angles masks applied to band 3. Masked pixels (not useful) are in dark.

3. Results.

3.1 Cloud/shadow/snow/haze-mask

The Round Robin Data guidelines recommend the selection of thresholds as restrictive as possible, taking into account the available data in order to avoid noise in the time series. If we choose loose thresholds (e.g., mask set on less than 70% R-R confidence level) the pixels in the time series will consequently show high variation from scene to scene. This condition implies that some remaining contamination in the image affects the data values. On the other hand, strict thresholds (mask set on less than 30%) are chosen, consequently the number of useful observation decreases. Table 1 shows the frequency of images with available pixels according to different thresholds in the cloud/shadow/snow/haze-mask for 2005. When the mask is set to less than 30% the number of available images decreases to zero.

Figure 3 shows the difference between the three thresholds. Accordingly, we decided to use a moderate threshold (50%) in order to increase the number of available data and minimize noise in the time series.

Table 1. Frequency of images with available pixels according to different thresholds in the cloud/shadow/snow/haze-mask for 2005.

	Loose threshold (70%)	Moderate threshold (50%)	Strict threshold (30%)
Percentage of images with more than 50% of useful data	18.75%	16.70%	0%
Percentage of images with more than 70% of useful data	7.63%	6.25%	0%

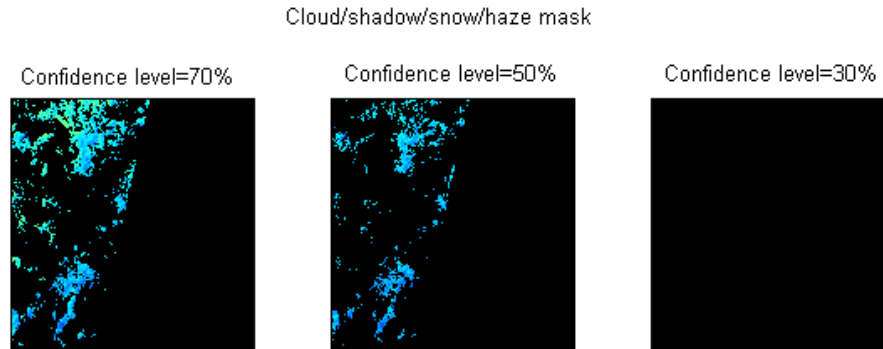


Figure 3. Example of the applied confidence levels for the cloud/shadow/snow/haze mask. Masked pixels (not useful) are in dark.

3.2 MIR band (3.7 μm)

The burned area detection algorithm used by INPE in this R-R exercise is based on the 3.7μm channel day-time images. The 3.7 μm AATSR channel is highly sensitive to radiation emitted at temperatures from 500K to 1000K (Mota et al., 2006), and also to reflected solar radiation. The low saturation level of the 3.7μm AATSR channel around 311K considerably reduces its application over bright regions, such as burning or recently burned areas.

Figure 4 shows an example of the saturation problems found in the day-time 3.7μm channel. Burned areas and sparsely or no vegetated areas (see the RGB image), which present higher temperatures, are flagged as no-data in 3.7μm channel, due to sensor saturation. Along the whole period (from January 2005 to December 2006) this problem occurs frequently, and prevents INPE's algorithm to accurately discriminate burned areas.

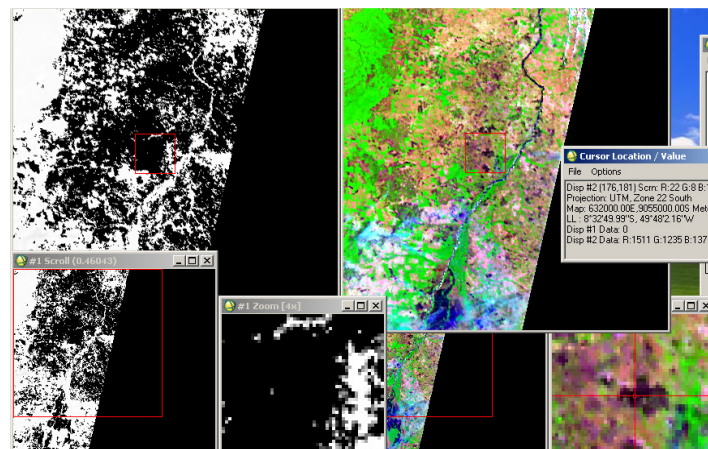


Figure 4. Comparison between the 3.7μm channel (left panel) and a RGB of SWIR, NIR, RED channels (right panel) from 19/09/2005. Black pixels indicate no-data.

Figure 5 presents the total number of images covering the study area (left panel: 2005 year, right panel: 2006 year). Around 30% of the images cover less than 10% of the study area. In addition, the MIR channel saturation is responsible for an increase of 5% in the images having 90-100% of no-data. Taking into account both problems, 62.5% of the 144 images have less than 50% of valid data. Considering also the cloud/shadow/show/haze occurrences, the number of images not useful increases to 81.5%. Finally, after applying the angles thresholds, we are left with only 20 images with more than 50% of valid data in 2005. Figure 6 summarizes the above mentioned drawback by presenting the map of the study area with the number of days containing valid MIR data, after applying the thresholds described. INPE' burned area algorithm was developed to detect changes in the (V,W) burned index time series. Since few valid data are available along the whole period, the algorithm simply cannot be used.

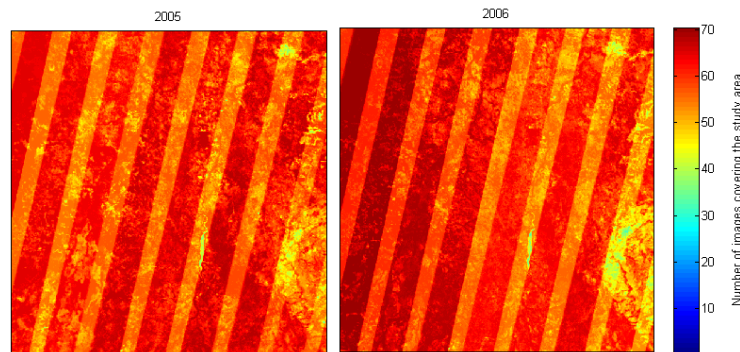


Figure 5. Number of images covering the study area. Left panel: 2005 year. Right panel: 2006 year

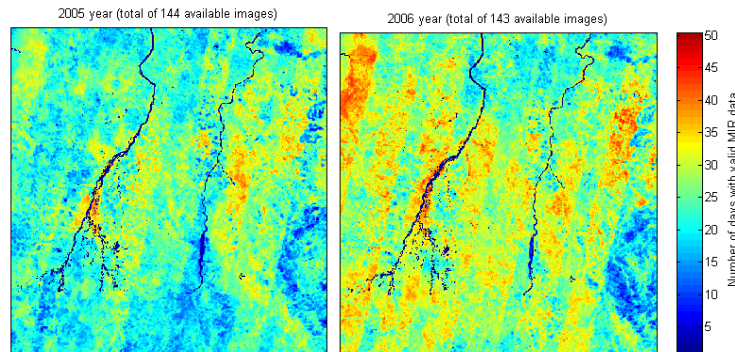


Figure 6. Map of the study area showing the number of days with valid MIR data after applying the thresholds described above. Left panel, 2005; Right panel, 2006. The small areas and the low number of days available for practical use should be noticed.

3.3 SWIR band (1.6 μ m)

Taking into account AATSR MIR channel data limitations we have tried instead to use the shortwave-infrared (SWIR), around 1.6 μ m, as a surrogate of the MIR channel, since the spectral response to fire scars in the SWIR domain is similar to that observed in the MIR region (Kaufman and Remer, 1994). In addition, the SWIR domain, as the MIR, appears adequate for monitoring the land surface during fire episodes because it is largely unaffected by the presence of aerosols. However, as already mentioned, the “V,W” burned index was firstly designed for MODIS sensor characteristics of channels 2 (near infrared, around 0.8 μ m)) and 20 (middle-infrared – daytime, around 3.9 μ m), and no previous validation approach was conducted to SWIR region.

Figure 7 presents the study area with the number of days containing valid SWIR data after applying the thresholds described (such as in Figure 6).

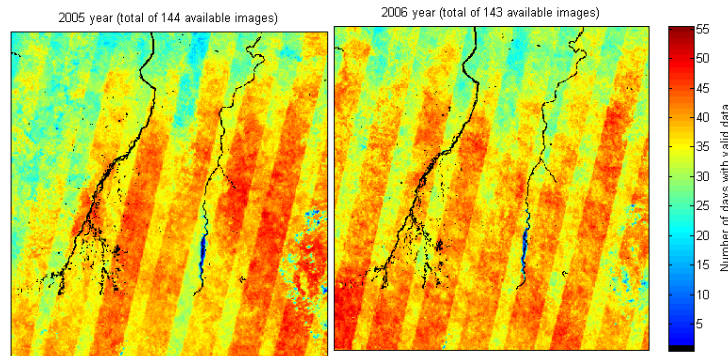


Figure 7. Same as Figure 6, but for SWIR channel. Left panel: 2005. Right panel: 2006.

Although more valid data is available in the case of the SWIR channel because saturation is very rare, problems remain in the dataset. For instance, Figure 8 shows another drawback found in the data set, SWIR channel does not presents any valid data (left panel), while NIR and RED channels apparently do not have any problem

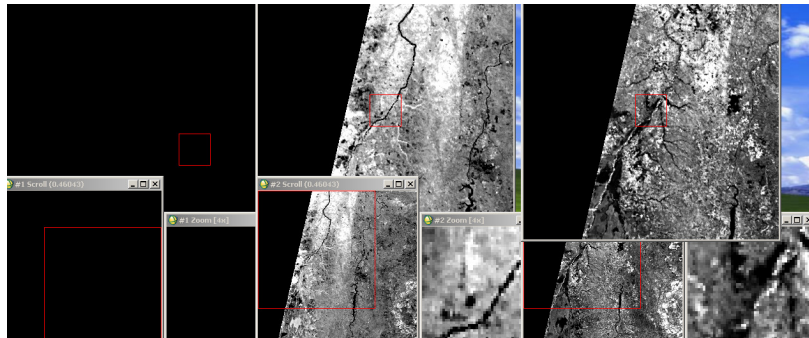


Figure 8. Comparison between the 1.6µm channel (left panel), 0.87µm channel (middle panel) and 0.6µm channel (right panel). Black pixels denote no-data.

3.4 Analysis of the results

An analysis of the result was conducted for INPE’s algorithm using the SWIR AATSR band. The reference dataset is formed by fire perimeters mapped from Landsat TM imagery (223/67) following the protocol explained in the Product Validation Plan (Chuvieco et al., 2011b), as well as by the hotspots detected by the MODIS sensor.

Figure 9 presents the difference in days between the dates detected by INPE’s BA algorithm and the date of MODIS hotspots in the R-R database. It is clear that most of the scars are wrongly dated by our algorithm. This behavior is mostly due to the reduced number of available AATSR data along the period of the study. The existence of values in the negative side of the scale is an indication of a continuous level of commission errors.

Figure 10 shows the comparison between the location of the scars detected by our algorithm and, respectively, the location of MODIS hotspots and the fire pixels at BDQ (INPE’s database of fire pixels) using all satellites, not only MODIS. Figure 11 shows the comparison between the locations of the scars detected by our algorithm (red polygons) for the whole year of 2005 and the R-R ground truth (green) for the period between 19-Jul-2005 and 22-Aug-2005. In both cases, the scarcity of the data impairs the good performance of the algorithm.

It is worth noting that these results were generated by using SWIR band as a surrogate of MIR band. This alternative probably also contributes to the poor performance of the algorithm, since no previously studies have yet shown the accuracy of “V,W” burned index with the SWIR region.

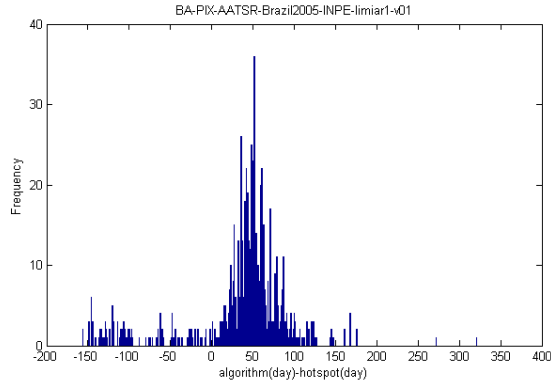


Figure 9. Difference in days between the dates detected by INPE’s algorithm and the date of MODIS hotspots.

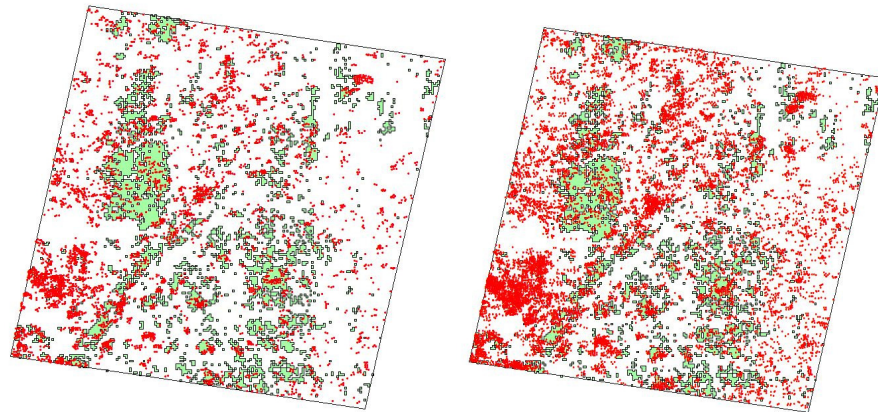


Figure 10. Comparison between the locations of the scars detected by our algorithm (green polygons) and MODIS hotspots (red points - left) and for the fire pixels in the BDQ (all satellites, not only Modis) (red points - right).

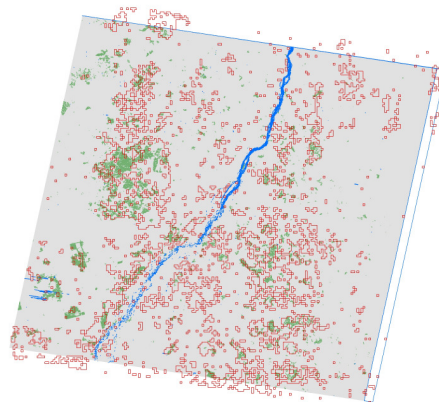


Figure 11. Comparison between the locations of the scars detected by our algorithm (red polygons) for the whole year of 2005 and the R-R ground truth (green) for the period between 19-Jul-2005 and 22-Aug-2005.

4. Conclusions

We observed that the information contained in the 3.7 μm AATSR channel offered large variations from date to date due to sensor saturation, impairing the application of our algorithm. In addition we have observed that the provided time series frequently does not contain information of the whole study area. Moreover, the cloud/haze/snow/shadow mask considerably limitsthe performance of the algorithm. With loose thresholds pixels in the time series show high variation from scene to scene. This fact implies that maybe some remaining contamination in the image is affecting the values. On the other hand, with strict thresholds (mask set on less than 30%) the number of available observation decreases considerably.

Due to the problems in the MIR band we have tried to use SWIR band as a surrogate of MIR one. Although more valid data is available in the case of the SWIR, problems remain in the dataset and no valuable result was obtained.

Acknowledments

This work was developed with the support of Fundação de Amparo à Pesquisa do Estado de São Paulo (FAPESP) under scholarship 2010/19712-2, and also from CNPq-PCI-INPE-CCST #551006/2011-0 e CNPq-AP #309765/2011-0 processes, and the GIZ Jalapão Project. The authors thank Silvia de Jesus and Ana Lia Lopes for the burned scar Landsat image analysis.

References

- Chuvieco, E. et al. ESA CCI ECV Fire Disturbance - Data Access Requirements Document: Fire_cci_Ph1_UAH_DOC_D1_3_DARD_v1_7.pdf, https://www.esa-fire-cci.org/webfm_send/189, 2011a.
- Chuvieco, E. et al. ESA CCI ECV Fire Disturbance - Product Validation Plan: Fire_cci_Ph1_UAH_D2_1_PVP_v3_1.pdf, https://www.esa-fire-cci.org/webfm_send/241, 2011b.
- Kaufman, Y. J., Remer, L. Detection of forests using mid-IR reflectance: An application for aerosol studies. *IEEE Transactions on Geoscience and Remote Sensing*, v. 32(3), p. 672–683, 1994.
- Libonati, R., DaCamara, C.C., Pereira, J.M.C., Peres, L.F. Retrieving middle infrared reflectance for burned area mapping in tropical environments using MODIS. **Remote Sensing of Environment**, v. 114, p. 831–843, 2010.
- Libonati, R.; DaCamara, C.C. ; Pereira, J.M.C.; Peres, L. F. On a new coordinate system for improved discrimination of vegetation and burned areas using MIR/NIR information. **Remote Sensing of Environment**, v. 115, p. 1464-1477, 2011.
- Mota, B. et al. Screening the ESA ATSR-2World Fire Atlas (1997–2002). **Atmos. Chem. Phys.**, v. 6, p. 1409–1424, 2006.